Heat Capacity of Silver Sulfide

C. M. PERROTT AND N. H. FLETCHER

Department of Physics, University of New England, Armidale, N.S.W. 2351, Australia

(Received 21 October 1968)

The heat capacity of silver sulfide has been measured over the range 50°–400°C using an adiabatic calorimeter. The heat capacity of the α form, stable between 177° and about 600°C, is anomalous and has a form typical of an order–disorder transition with critical temperature at 350°C. If the sample deviates from stoichiometry by as little as one mole percent in either direction, its heat capacity is near normal at about 20 cal/mole·°C throughout the range of measurement. An interpretation of these results in terms of lattice disorder is suggested.

I. INTRODUCTION

A program of study of the physical properties of partially disordered solids was commenced with a calorimetric investigation of the high-temperature (α) phase of silver iodide.[1–3] This resulted in the identification of a rather complex order–disorder transition in stoichiometric silver iodide, while samples which deviate from stoichiometry by as little as one mole percent in either direction were found to have properties consistent with the silver ions being in a state of essentially complete long-range disorder over the entire temperature range of existence of α-AgI (150°–555°C). In this paper, we report a similar investigation of silver sulfide between 50° and 400°C, using the adiabatic calorimeter previously described.[1]

Investigations by Kracek[4] and Djurle[5] have elucidated the phase diagram shown in Fig. 1. There are three solid phases of silver sulfide, all of which are stable over a narrow range of compositions. The low-temperature phase, called either Ag$_2$S III or β-Ag$_2$S, has a monoclinic unit cell (C_{2h}^5 or $P2_1/n$) with lattice parameters $a = 9.53$ Å, $b = 6.92$ Å, $c = 8.28$ Å, and $\beta = 124°$ at room temperature.[5–7] At $177.8° \pm 0.7°$C in the presence of excess sulfur and $176.3° \pm 0.5°$C with excess silver, β-Ag$_2$S transforms to α-Ag$_2$S (or Ag$_2$S II) which is stable at temperatures up to $622° \pm 3°$C in excess sulfur and $586° \pm 3°$C in excess silver. The phase α-Ag$_2$S has a disordered structure analogous to that of α-AgI and exists over a similar temperature range. The sulfur ions occupy a body-centered cubic lattice, while the four silver ions of the unit cell are statistically distributed over the 42 equipoints of the space group $Im3m$ (Fig. 2),

$$(000, \tfrac{1}{2}\tfrac{1}{2}\tfrac{1}{2}) +$$

$$6(b): \quad (\tfrac{1}{2}, 0, 0) \curvearrowright$$

$$12(d): \quad \pm(\tfrac{1}{2}, 0, \tfrac{1}{4}) \curvearrowright$$

$$24(h): \quad \pm(\tfrac{5}{8}, \tfrac{3}{8}, 0) \curvearrowright, \pm(\tfrac{5}{8}, \tfrac{5}{8}, 0) \curvearrowright.$$

According to Rahlfs,[8] the various sites have the following occupation probabilities at 250°C: (d) sites $\tfrac{1}{8}$ and both (b) and (h) sites $\tfrac{1}{12}$. There is no available data on the variation of these occupation probabilities with temperature or composition. Conductivity measurements have shown that α-Ag$_2$S has an electronic conductivity[9] of ~ 500 Ω^{-1} cm^{-1} and an ionic conductivity[10–12] of ~ 2 Ω^{-1} cm^{-1}, which increases with in-
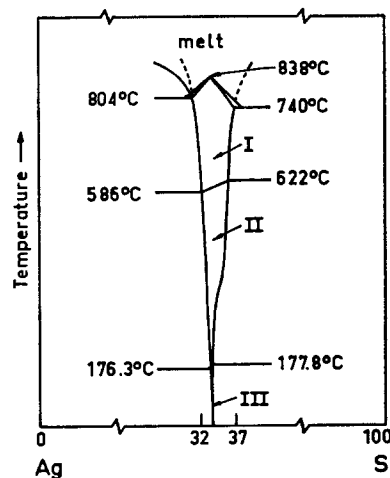

FIG. 1. Part of the phase diagram of the system Ag–S, showing the phases of the compound Ag$_2$S and the dependence of the transformation temperature on stoichiometry (after Kracek[4]).

creasing temperature. On the other hand, α-AgI has an ionic conductivity of about the same magnitude but an electronic conductivity at least four orders of magnitude smaller.[9] This difference in electronic conductivity is very much what would be expected if such conductivity is due to electron motion in the conduction band. The black, almost metallic appearance of α-Ag$_2$S suggests that its optical band gap is $\lesssim 1$ eV in comparison with ~ 4 eV in α-AgI and, in addition, the separation of Ag$^+$ ions in α-Ag$_2$S is so much less than in α-AgI that the conduction band would be much broader and electron mobility correspondingly higher.

[1] C. M. Perrott and N. H. Fletcher, J. Chem. Phys. **48**, 2143 (1968).

[2] C. M. Perrott and N. H. Fletcher, J. Chem. Phys. **48**, 2681 (1968).

[3] C. M. Perrott and N. H. Fletcher, J. Chem. Phys. (to be published).

[4] F. C. Kracek, Trans. Am. Geophys. Union **27**, 364 (1946).

[5] S. Djurle, Acta Chem. Scand. **12**, 1427 (1958).

[6] B. J. Skinner, Econ. Geol. **61**, 1 (1966).

[7] L. S. Ramsdell, Am. Mineralogist **28**, 401 (1943).

[8] P. Rahlfs, Z. Physik. Chem. **B31**, 157 (1935).

[9] W. Jost; *Diffusion in Solids, Liquids and Gases* (Academic Press Inc., New York, 1960), pp. 345–8.

[10] H. Okazaki, J. Phys. Soc. Japan **23**, 355 (1967).

[11] S. Miyatani, J. Phys. Soc. Japan **10**, 786 (1955); **13**, 341 (1958); **15**, 1586 (1960).

[12] I. Yokota, J. Phys. Soc. Japan **16**, 2213 (1961).

The highest temperature phase, Ag_2S I, which melts congruently at 838°C has also been called α-Ag_2S because of its disordered structure. For clarity, we will designate this phase α'-Ag_2S, pointing out that there is no analogous phase of AgI but that the high-temperature phase α-Cu_2S has identical structure, as is indicated by the complete solid solubility of $(Ag, Cu)_2S$.[13] The phase α-Cu_2S has a cubic close-packed array of anions[14] while the x-ray data obtained at $\sim$90°C showed 9/10 of a cation statistically distributed over 24 equipoints of the space group $Fm3m$ clustered near the center of each of the sulfur tetrahedra,[14] indicating that the material studied was nonstoichiometric. The heat capacity of this phase has not been measured and we will not discuss its properties further.

II. EXPERIMENTAL

A. Preparation of Samples

Silver sulfide was precipitated at room temperature from aqueous solutions of analytical reagent-grade silver nitrate and sodium sulfide. The dense black precipitate was flocculated, washed in a filtering crucible, and dried at $\sim$90°C in an air oven. The fine powder was then compacted into the stainless steel sample holders previously described,[1] which were then sealed by argon arc welding. Nonstoichiometric samples were prepared by dispersing either small flakes of silver metal or powdered sulfur through the Ag_2S powder before compaction. After sealing into the sample holders, the samples were annealed at $\sim$500°C for as long a period of time as was necessary to obtain uniform nonstoichiometric samples. The samples comprised 0.1 moles and were compacted to at least 95% of the crystalline density.
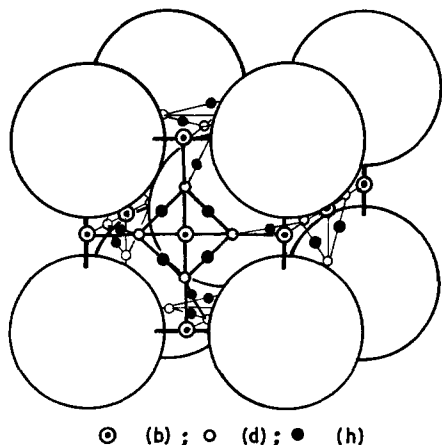

FIG. 2. Schematic drawing of the structure of α-Ag_2S. The large spheres represent sulfide ions, while the remaining sites are available to silver ions.

$\odot$ (b) ; $\circ$ (d) ; $\bullet$ (h)

[13] G. M. Schwartz, Econ. Geol. 30, 128 (1935).
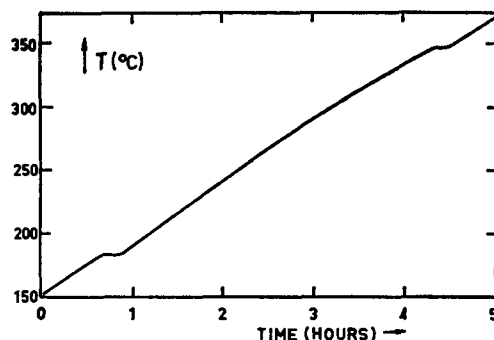[14] N. Morimoto and G. Kullerud, Am. Mineralogist 48, 110 (1963).

FIG. 3. A typical heating curve for stoichiometric silver sulfide, showing the phase transition β-Ag_2S to α-Ag_2S at 180°C and the critical temperature for disordering, 350°C.

B. Results for Annealed Samples

A typical heating curve for stoichiometric silver sulfide is shown in Fig. 3. The phase transformation β-Ag_2S to α-Ag_2S at about 180°C is shown by the abrupt fall in heating rate at that temperature. From a knowledge of the time taken to complete the transformation and the constant power supplied to the sample, the latent heat of transformation may be determined. For stoichiometric material, the latent heat was found to be

$$\delta H = 950 \pm 100 \text{ cal/mole.}$$

The corresponding entropy change at the transition is then,

$$\delta S = 2.1 \pm 0.2 \text{ cal/mole} \cdot °C.$$

These values are in good agreement with the values $\delta H = 960$ cal/mole and $\delta S = 2.14$ cal/mole·°C previously reported.[15]

From Fig. 3, we see that there is another transition at 350°C, for which the latent heat and entropy change are found to be

$$\delta H = 600 \pm 100 \text{ cal/mole}$$

and

$$\delta S = 1.0 \pm 0.2 \text{ cal/mole} \cdot °C.$$

In the literature, however, we can find no reference to a phase change at this temperature and must therefore seek an alternative explanation of our observations.

The heat capacity for stoichiometric silver sulfide has been determined in the range 50°–400°C and is shown in Fig. 4, the absolute accuracy being estimated as $\pm$10%. The heat capacity of α-Ag_2S is anomalously high and increases rapidly with increasing temperature before a sudden fall to a near normal value $C_p = 22$ cal/mole for all temperatures above 350°C. This sudden change in the heat capacity has an associated latent heat and the curve of Fig. 4 is of the form one would expect if there were an order–disorder transition in α-Ag_2S with critical temperature at 350°C and a dis-

[15] International Critical Tables (McGraw-Hill Book Co., New York, 1930), Vol. 5, p. 188.
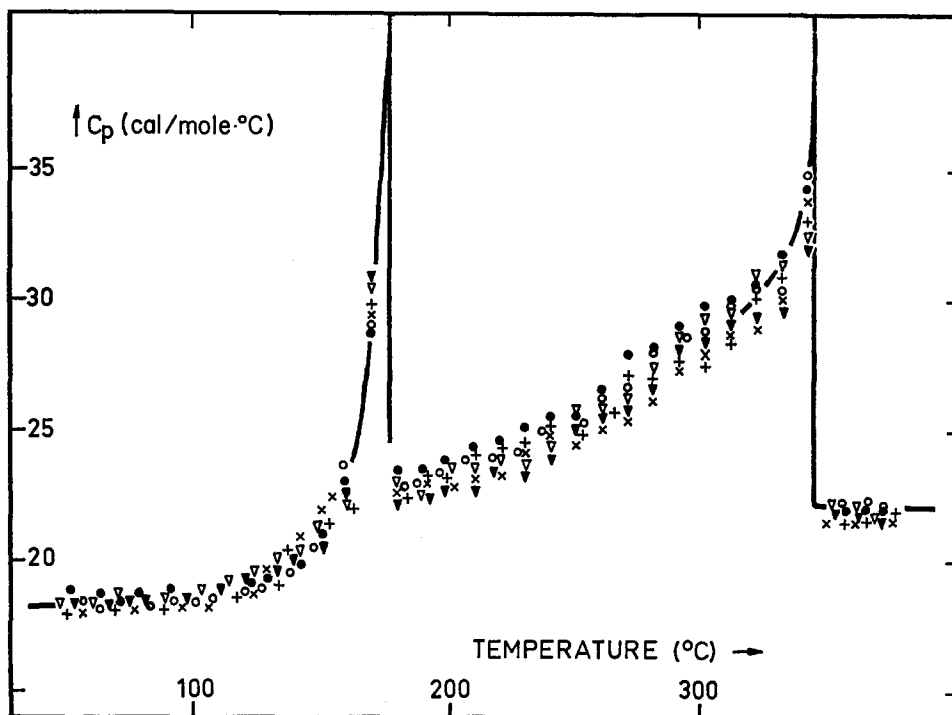
FIG. 4. Molar heat capacity of annealed stoichiometric silver sulfide. Different symbols are for different runs and samples.

continuous change in the long-range order parameter on disordering.

For small deviations from stoichiometry in the sample, the heat capacity was found to be constant from 180° to 400°C and equal to that of stoichiometric material above the order–disorder transition (Fig. 5). For the sample containing one mole percent excess silver, the latent heat of transformation β-Ag$_2$S to α-Ag$_2$S was found to be

$$\delta H = 1550 \pm 100 \text{ cal/mole}$$

with corresponding entropy change

$$\delta S = 3.5 \pm 0.2 \text{ cal/mole} \cdot {}^{\circ}\text{C}$$

These values are significantly higher than those for stoichiometric material and are in agreement with the value $\delta H = 1520$ cal/mole reported by Roy et al.,[16] while Kapustinski and Veselovskii[17] found that "γ-Ag$_2$S" had a heat capacity $C_p = 22$ cal/mole·°C over its range of existence 179°–570°C. From the value of this upper temperature limit, the phase diagram of Fig. 1 suggests that their γ-Ag$_2$S was in fact silver-rich α-Ag$_2$S and, if this is true, their results are seen to support our own. For fully annealed samples, no latent heat was observed at 350°C and the results are consistent with the state of long-range disorder of the silver ions being essentially complete at all temperatures above 180°C.

The sulfur-rich samples were found to have the same properties as the silver-rich samples. These results are essentially the same as those obtained with silver iodide, except that, for silver iodide, no increase in latent heat of transformation was observed on doping. For exactly the same reasons as for the silver iodide case, we may show that the decrease in heat capacity of silver sulfide on incorporation of excess silver or excess sulfur into the structure cannot be explained in terms of a simple reaction between the Ag$_2$S and the doping agent. Rather, the calorimetric and structural data can only be explained if we assume that some process occurs whereby the disordering of the silver ions becomes complete immediately above the 180°C phase change.

C. Conversion to Heat Capacity at Constant Volume

Before proceeding to develop a theoretical model of this order–disorder transition, we must convert our experimental results C_p to the more theoretically significant heat capacity C_v.

[16] R. Roy, A. J. Majumdar, and C. W. Hulbe, Econ. Geol. **54**, 1278 (1959).
[17] A. F. Kapustinski and B. K. Veselovskii, J. Phys. Chem. (USSR) **11**, 68 (1938).

TABLE I. Corrections $C_p - C_v$ for α-Ag$_2$S at various temperatures.

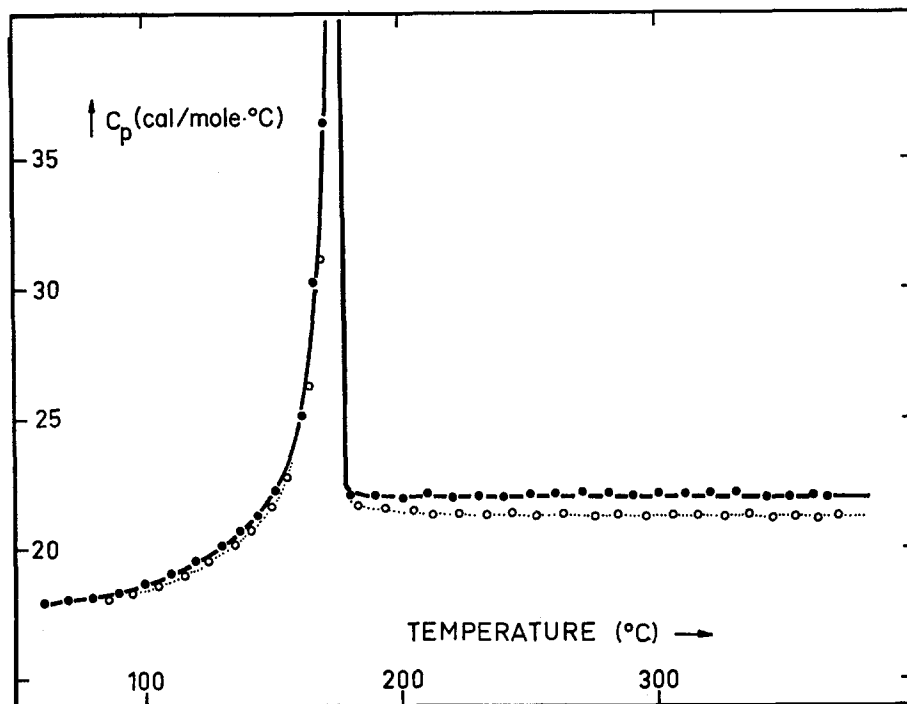| T(°C)	200	250	300	350	400	450	500
$C_p - C_v$ (cal/mole·°C)	1.69	1.88	2.07	2.22	2.40	2.60	2.75

FIG 5. Molar heat capacity of annealed nonstoichiometric silver sulfide. ●, 1 mole % excess silver; ○, 1 mole % excess sulfur.

It may be shown that[18]

$$C_v = C_p - TV_m(9\alpha_l^2/K), \qquad (1)$$

where T is the absolute temperature, V_m is molar volume, $\alpha_l = (a_0)^{-1} (\partial a_0/\partial T)_p$ is the coefficient of linear expansion, and $K = V^{-1}(\partial V/\partial P)_T$ is the compressibility. The values of V_m and α_l may be obtained from the temperature dependence of the lattice parameter[5,8] a_0 (4.870 Å at 189°C, increasing to 4.926 Å at 500°C), while the compressibility of α-Ag$_2$S has not been measured and we must make an estimate using the value $K = 2.7 \times 10^{-12}$ cm^2/dyn which applies to β-Ag$_2$S at room temperature.[19] The values of $C_p - C_v$ thus calculated are given in Table I and are seen to be significant, although they do not change the general pattern of behaviour seen in Figs. 4 and 5.

III. THEORY: STOICHIOMETRIC α-Ag$_2$S

The structure model which we propose for stoichiometric α-Ag$_2$S is as follows. In a crystal containing $2N$ silver ions and N sulfur ions, there are $3N$ crystallographically equivalent sites of the type (b) for silver ions. Each (b) site is surrounded by a cluster of (h) and (d) sites, of which its share is four (h) and two (d) sites. Each such cluster is then crystallographically equivalent. We are thus faced with the problem of distributing $2N$ silver ions and N silver ion vacancies over a total of $3N$ equivalent sites, each site being not a simple potential well but a more complex well representing the cluster. Because of the relatively tight

[18] F. Seitz, *The Modern Theory of Solids* (McGraw-Hill Book Co., New York, 1940), p. 137.
[19] Reference 15, Vol. 3, p. 50.

packing of the structure, the distribution cannot be made on an independent particle basis. In fact, before a silver ion can be placed on any site, it is necessary to displace one or both of its neighboring sulfur ions from their perfect lattice positions. This displacement affects the potentials of all neighboring sites and the ordering or disordering of the silver ions and vacancies upon the sites of their lattice may be expected to be a cooperative phenomenon. We will now describe the mathematical treatment necessary to calculate the heat capacity of the silver ions.

For simplicity we take the lattice vibrations to be independent of the configurations of the silver ions on the lattice sites, so that we may split the partition function into configurational and vibrational factors. The thermodynamic functions of the system are then obtained by summing the corresponding functions evaluated separately for the two factors.

A. Configurational Heat Capacity of Ag$^+$ Ions

The configurational factor of the partition function may be written

$$Z(T, s_i) = \sum_m \exp(-W_m/kT), \qquad (2)$$

where T denotes the absolute temperature, s_i is a suitably defined set of parameters specifying the state of order of the alloy, and k is the Boltzmann constant. W_m represents the configurational energy of the state m, with the summation extending over all states m corresponding to a given ordering s_i.

Considering the silver lattice of α-Ag$_2$S, we have an AB$_2$ "alloy" comprising $2N$ silver ions (designated B)
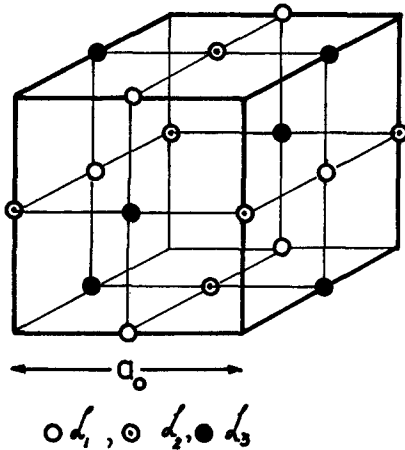
FIG. 6. The three equivalent sublattices available to silver ions. Each symbol represents a cluster of potential wells.

and N silver ion vacancies (designated A) distributed over $3N$ sites of the lattice shown in Fig 6, which has been divided into three interpenetrating body-centered cubic sublattices $\mathcal{L}_i$ ($i=1, 2, 3$) each having lattice parameter a_0. The mathematics describing the disordering of this alloy has already been presented in detail in connection with α-AgI[2,3] and no attempt will be made here to repeat this. The cation structure of Ag_2S is simply the dual of that of AgI in that the roles of silver ions and silver ion vacancies are interchanged in the two materials. In the interests of clarity in the following sections we shall, however, restate the physical assumptions involved in the calculation and write down the equations for the reduced temperature τ (defined in the detailed treatment) and configurational heat capacity.

The theory is a Bragg–Williams zero-order approximation in which it is assumed that the symmetry of distribution of the silver ions is determined largely by the symmetry of the body-centered cubic lattice of sulfide ions. This seems logical in view of the fact that it is the sulfide lattice which gives the material its mechanical characteristics. The proposed structure at low temperatures is therefore one in which the silver ions occupy two of the three bcc sublattices leaving the other one unoccupied. This ordered state has tetragonal
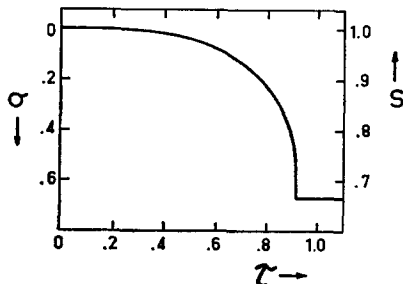

FIG. 7. Equilibrium values of the ordering parameters σ and s as a function of reduced temperature τ.

symmetry with a c/a ratio close to unity. Although the close packing of the structure might be expected to give rise to a c/a ratio different from unity, the preferential occupation of (d) and (h) rather than (b) sites in fact causes distortions of the sulfide lattice along all three axial directions.

From the symmetrical relationship between the sublattices (Fig. 6) and the nature of the ordered state, we propose that two of the sublattices will have the same occupation probability, s (say), while the other one will have occupation probability $\sigma = 1 - 2s$. Using this relationship between the order parameters, we find that the reduced temperature

$$\tau = kT/v \qquad (3)$$

and the equilibrium value of σ are related by the equation

$$\tau = \frac{2(2-3\sigma)}{\ln\{[(1-\sigma)/\sigma][(2-\sigma)/\sigma]\}}. \qquad (4)$$
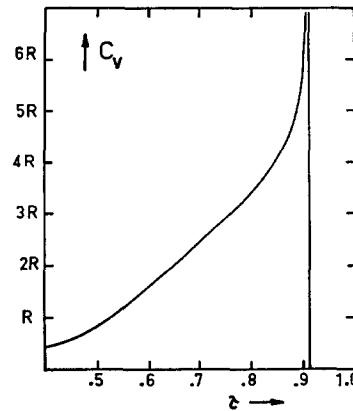

FIG. 8. Configurational specific heat of silver ions as a function of reduced temperature τ.

The symbol v represents the ordering energy of the alloy. Solving this equation, we find that the equilibrium values of σ and s vary with reduced temperature in the manner of Fig. 7, from which it is seen that the silver ions disorder progressively as the temperature is increased until a critical temperature $\tau = 0.915$ is reached, where a discontinuous change occurs in the degree of disorder. At all higher temperatures $s = \sigma = \frac{2}{3}$ and the silver ions are fully disordered. The molar configurational specific heat may be determined from the equation,

$$C_v{}^{\text{config}} = R(\partial/\partial\tau)[\sigma(4-3\sigma)] \qquad (5)$$

and the calculated variation of σ with τ, and is plotted in Fig. 8. It represents the major contribution to the anomalous heat capacity of α-Ag_2S.

B. Vibrational Heat Capacity of Ag^+ Ions

The specific heat contributed by the vibrational factor of the partition function may be calculated by

the same method as that used for α-AgI.[3] The appropriate potential for the cluster is

$$V(r, \theta, z) = V(r, \theta) + V(z), \qquad (6)$$

where

$$V(z) = Ez^2/a^2 \quad \text{for} \quad -\infty \leq z \leq \infty \qquad (7)$$

and, if $r \leq r_0$,

$$V(r, \theta) = E_b + \epsilon r^2/r_0^2 \qquad (8)$$

where, if $r \geq r_0$,

$$V(r, \theta) = V(\theta) + (E_b + \epsilon)(r - 2r_0)^2/r_0^2, \qquad (9)$$

and

$$V(\theta) = (\epsilon + E_h)(\theta - \tfrac{1}{2}n\pi)^2(8/\pi)^2$$

$$\text{for} \quad \tfrac{1}{2}\pi(n - \tfrac{1}{4}) \leq \theta \leq \tfrac{1}{2}\pi(n + \tfrac{1}{4})$$

$$= E_h + \epsilon[\theta - \tfrac{1}{2}\pi(n + \tfrac{1}{2})]^2(8/\pi)^2$$

$$\text{for} \quad \tfrac{1}{2}\pi(n + \tfrac{1}{4}) \leq \theta \leq \tfrac{1}{2}\pi(n + \tfrac{3}{4})$$

$$\text{where} \quad n = 0, 1, 2, 3. \qquad (10)$$

The fact that each (d) site is shared by two clusters is included by assigning statistical weight $\tfrac{1}{2}$ to $V(\theta)$ in the range $\tfrac{1}{2}\pi(n - \tfrac{1}{4}) \leq \theta \leq \tfrac{1}{2}\pi(n + \tfrac{1}{4})$. The heights of the (b) and (h) sites with respect to an arbitrary zero set at the base level of the (d) sites are E_b and E_h, respectively, and, from Rahlfs'[8] data at 250°C, they are both equal to 425 cal/mole. For any reasonable assumption about the energy ϵ, we find that the vibrational heat capacity of the $2N$ silver ions in a mole of α-Ag$_2$S is actually less than the classical value $6R$ by an amount $1.5R$ at 500°K, $1.4R$ at 650°K, and $1.1R$ at 800°K.

C. Vibrational Heat Capacity of S^{2-} Ions

Each sulfide ion may be regarded as vibrating in a harmonic well whose position in space is determined by the surrounding configuration of silver ions. Thus, the sulfide ions have a normal vibrational heat capacity $3R$ plus some configurational heat capacity resulting from the entropy associated with the displacements of the potential wells. If each silver cluster was a simple site, each configuration of silver ions would specify a unique configuration of sulfide ions and the entropy would simply correspond to the entropy $k \ln g(s)$ associated with the number of arrangements of the silver ions over the sublattices. This is included in the configurational energy of the silver ions and does not give a further heat-capacity contribution through the sulfide ions. Since each cluster contains a silver ion distributed over a number of sites, the real positions of the sulfide ions for a given configurational state of the silver alloy will be uncertain and will depend upon the instantaneous positions of the silver ions in the clusters. To attempt to treat this problem mathematically would be pointless because it represents a higher order of approximation than that used for the AB$_2$ alloy and in fact we will neglect any heat capacity contribution from this cause,
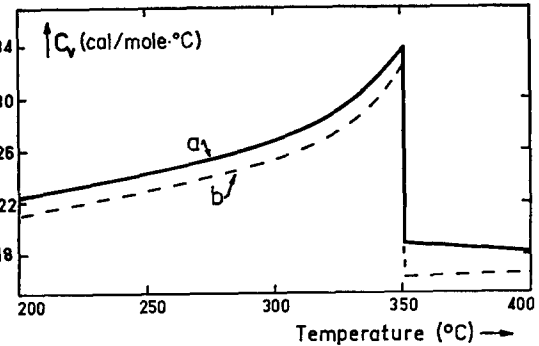
FIG. 9. Comparison of calculated heat capacity for α-Ag$_2$S with experiment. Curve a is the experimental curve and curve b is the theoretical curve.

assuming that the silver ions move from site to site within a cluster so rapidly that the sulfide ions only react to the average potential of the clusters.

D. Comparison with Experiment

The experimental curve of Fig. 4 and the results of Table I may be used to plot an experimental C_v versus temperature curve as in Fig. 9(a). Noting that the critical temperature $\tau = 0.915$ has been observed experimentally at 350°C, we can convert from reduced temperature to absolute temperature and add the various heat capacity contributions mentioned above to obtain the theoretical curve b of Fig. 9. Considering the elementary nature of the theory, the agreement between experiment and theory is remarkably close. The behavior above the critical temperature is a problem of short-range order between silver ions and at present we do not have enough experimental evidence or theoretical insight to formulate a description of the long-range disordered state existing above the critical temperature.

Since we do not have an adequate measure of the state just above the critical temperature and, indeed, only a rough idea of the situation just below the critical temperature, we cannot expect our present theory to predict a satisfactory value of the latent heat associated with the disordering. In fact, the value calculated from the discontinuous change in σ and the corresponding entropy change for the silver ions is only 100 cal/mole. This may possibly be stretched to 200 cal/mole by considering entropy changes for the sulfide ions, but it is clear that our model will give but semiquantitative agreement with the observed latent heat of 600 cal/mole.

IV. CONCLUSIONS

From the experimental results and subsequent discussion, we conclude that the anomalous specific heat of α-Ag$_2$S is consistent with the occurrence of a rather complex order–disorder transition in the material with critical temperature for disordering at 350°C. The heat capacity below the critical temperature may be explained, with fair agreement, using a long-range

model of the disorder which was developed for the similar system α-AgI.

In the case of nonstoichiometric material, we have seen that deviation from stoichiometry by as little as one mole percent in either direction probably results in complete long-range disordering of the silver ions at all temperatures above the β-Ag$_2$S to α-Ag$_2$S phase transition. Just as we cannot describe the state of short-range order above the critical temperature in stoichiometric material, we cannot describe the state of the nonstoichiometric material, no do we have any firm idea as to how the critical temperature is quenched by the excess silver or excess silver vacancies. The same

dependence of heat capacity on stoichiometry was observed in α-AgI and is a further indication of the similarity between the two systems.

EPR Spectrum of Fe³⁺ in Synthetic Brown Quartz

L. M. MATARRESE, J. S. WELLS, AND R. L. PETERSON

National Bureau of Standards, Boulder, Colorado 80302

(Received 8 March 1968)

A detailed description is given of the EPR spectrum of Fe³⁺ in synthetic brown quartz (the so-called I center, presumed to be interstitial). There are three equally populated sites differing only in the orientation of their principal axes, which coincide with the three twofold axes of quartz. The values of the Hamiltonian parameters that fit the data best are: $g = 2.0039$, $C_{20}(\equiv D) = 734.3G$, $C_{22}[\equiv (6^{1/2}/2)\,|\,E\,|] = 401.7G$, $C_{40} = 2.52G$, $C_{44} = 1.40G$, where the C_{lm} are the coefficients of the Racah operators in the Hamiltonian. Lobes of the V_{22}, V_{42}, and V_{44} parts of the crystal-field potential point $0.7°$, $29.5°$, and $26.8°$, respectively, from the optic axis of quartz. The occurrence of irregular off-axis extrema of the line positions when the magnetic field is directed in the vicinity of the optic axis precludes the assignment of magnetic axes of the paramagnetic center in the usual way. All features of the spectrum are predicted accurately by computer calculations based on the derived Hamiltonian. Although the data are not conclusive evidence, they are believed to be more consistent with an assignment of the I center to a substitutional site.

I. INTRODUCTION

Our story begins with natural amethyst, a purple-colored quartz. Several years ago we began an investigation of the rich and bewildering EPR spectrum yielded by an amethyst crystal taken from a mineral collection. Suspecting that Fe³⁺ was the impurity responsible for the spectrum, we interrupted its study to examine the EPR spectrum of Fe³⁺ introduced into synthetic quartz crystals during growth. In these crystals, which are variously green and brown in color, we found an obvious Fe³⁺ spectrum that was quite different from the dominant EPR spectrum characteristic of amethyst, although traces of the latter could be found in some of the synthetic crystals. Our preliminary report[1] on this new spectrum attributed it to substitutional Fe³⁺ in three differently oriented but otherwise equivalent sites. This paper is a precise description of this spectrum. The paper directly following in this issue[2] supplements this

description with a report of our zero-field experiments on the same specimen. Details of the mathematical analysis of the spectrum have been published separately.[3]

The EPR spectrum of natural amethyst (NA) is indeed due to Fe³⁺ and has been well characterized by Hutton[4] and by Moore and his co-workers.[5] The chief differences between the dominant EPR spectra of NA and synthetic brown quartz (SBQ) are: a grossly unequal distribution of the Fe³⁺ ions among the three sites in NA, a much greater zero-field splitting (24 and 35 GHz) in NA than in SBQ (7 and 9 GHz), and a different orientation of the crystal-field axes, i.e., while both centers share the three twofold crystallographic axes of quartz as one of the crystal-field axes of each site, the crystal-field axes in the planes perpendicular to the twofold axes are rotated by an angle of 57° from the optic axis of quartz in the case

[1] L. M. Matarrese, J. S. Wells, and R. L. Peterson, Bull. Am. Phys. Soc. 9, 502 (1964).

[2] A. R. Cook and L. M. Matarrese, J. Chem. Phys. 50, 2361 (1969), following paper.

[3] R. L. Peterson, L. M. Matarrese, and J. S. Wells, Natl. Bur. Std. (U.S.), Tech. Note 372 (1969).

[4] D. R. Hutton, Phys. Letters 12, 310 (1964).

[5] T. I. Barry and W. J. Moore, Science 144, 289 (1964). T. I. Barry, P. McNamara, and W. J. Moore, J. Chem. Phys. 42, 2599 (1965).